Synthesis and conformational analysis of cyclic analogues of inverse γ-turns†

Morakot Kaewpet,[a] Barbara Odell,*[a] Michael A. King,[b] Biswadip Banerji,‡[a] Christopher J. Schofield*[a] and Timothy D. W. Claridge*[a]

Received 28th May 2008, Accepted 4th July 2008
First published as an Advance Article on the web 7th August 2008
DOI: 10.1039/b808954j

γ-Turn analogues comprising a modified dipeptide constrained in an eleven-membered ring were prepared by alkene metathesis and analysed by NMR and molecular modelling studies. The results reveal that some of the cyclic analogues form inverse γ-turns and preferentially adopt conformations determined by the identity of the incorporated amino acid residues and the nature of the constraining linker (*E*/*Z*-alkene or alkane).

Introduction

Many pharmaceutical and biological probes may be viewed as conformationally constrained analogues of peptides (for reviews see ref. 1–5). Significant attention has been focused on analogues of β-turns, but less work has been directed towards analogues of γ-turns, which involve three residues. In γ-turns (Fig. 1a), the carbonyl oxygen of the first residue (*i*) may be hydrogen bonded to the amide NH of the third residue (*i*+2), giving rise to a seven-membered ring. The term 'open γ-turn' is used for situations where no formal intramolecular hydrogen bond is present. There are two types of γ-turns, classic and inverse, defined according to their ϕ and ψ torsion angles.[6] The classic and inverse γ-turns differ in that the main-chain atoms of the two forms are related by mirror symmetry. It has been proposed that inverse γ-turns are intermediates in protein folding and stabilise β-strands before they become β-sheets.[7]

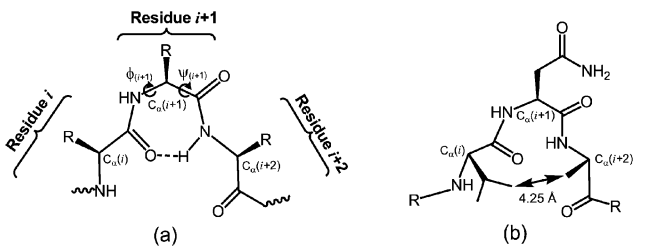

Fig. 1 (a) Structure of the γ-turn; (b) view of the 'open γ-turn' of the VNA residues (802–804) of the C-terminal transcriptional activation of hypoxia inducible factor-1α (HIF-1α) in the binding conformation observed when in complex with factor inhibiting HIF (FIH), an asparaginyl hydroxylase.[8]

γ-Turns also occur in receptor–peptide ligand interactions,[9] and in enzyme–substrate complexes.[10–12] One example of the latter occurs in the substrate conformation adopted by the substrate in the complex formed between factor inhibiting hypoxia inducible factor-α (FIH), a dimeric asparaginyl hydroxylase, and its substrate, the C-terminal transcriptional activation domain of HIF-1α (hypoxia inducible factor-1α).[8] In a crystal structure of an FIH–HIF-1α-Fe(II)-2-oxoglutarate complex, the residues Val802-Asn803-Ala804 (VNA) of HIF-1α adopt an inverse γ-turn with dihedral angles, $\phi(i+1)$ of −78° and $\psi(i+1)$ of 61° and a $C_\alpha(i)$ to $C_\alpha(i+2)$ distance of 5.5 Å[8] (Fig. 1b). This γ-turn structure positions the Asn803 β-methylene adjacent to the active site iron of FIH in preparation for asparaginyl hydroxylation.

FIH has also recently been reported to catalyse the hydroxylation of human ankyrin repeat domain proteins.[13] Fragments of ankyrin repeat domain proteins were shown to bind to FIH in an identical manner to HIF-$1\alpha_{786-826}$ in the active site region, *i.e.* with an inverse γ-turn.[14] This observation was interesting because crystallographic analyses of ankyrin repeat domain proteins normally comprise repeats of well defined helix-turn-helix motifs, that would not likely bind to FIH in a catalytically productive manner.

FIH[15–17] is one of the HIF-α hydroxylases that act as oxygen sensors in humans; these enzymes are therapeutic targets with a view to inducing the hypoxic response for therapeutic effect (for review see ref. 18). We are interested in inhibiting the HIF hydroxylases and in understanding the dynamics of the FIH–HIF-1α interaction. One strategy to inhibit FIH would be using conformationally restrained cyclic analogues of the γ-turn adopted by the HIF-1α substrate at the FIH active site. There are no reports on how the nature of the linker used to form a cyclic analogue can alter the conformation of γ-turn analogues. To address this question, we targeted the synthesis of potential γ-turn analogues constrained by an aliphatic chain. We report the synthesis and analysis of conformationally constrained γ-turn analogues based on an eleven-membered ring structure generated by alkene metathesis. NMR and modelling studies reveal that the cyclic template can stabilise a γ-turn conformation. Importantly,

[a]*Chemistry Research Laboratory, Department of Chemistry, University of Oxford, 12 Mansfield Road, Oxford, UK OX1 3TA. E-mail: barbara.odell@chem.ox.ac.uk, christopher.schofield@chem.ox.ac.uk, tim.claridge@chem.ox.ac.uk.; Fax: +44 1865275674; Tel: +44 1865275625*

[b]*CADD Group, UCB Celltech, 208 Bath Road, Slough, UK SL1 3WE; Fax: +44 1753536632; Tel: +44 1753534655*

† Electronic supplementary information (ESI) available: ^{1}H NMR spectra of **Z-4b**, **E-4b**, **5** and **10**; tables of ^{1}H NMR data for **Z-4b** and **E-4b**, **5** and **10**; selected NOEs for conformer A of **Z-4b**, conformers A, B and C of **E-4b**, conformer A of **5** and conformer B of **5**, relevant NOEs from the NOESY spectrum of **10** and observed ^3J coupling constants and calculated dihedral angles of **10**. See DOI: 10.1039/b808954j

‡ Current address: Chemical Synthesis Laboratory@Biopolis, Institute of Chemical and Engineering Sciences (ICES), Agency for Science, Technology, and Research (A*STAR), 11 Biopolis Way, The Helios Block, #03–08, Singapore 13866.

we find that the nature of the linker sequence (*E*- or *Z*-alkene) can significantly alter the observed conformations in solution.

Results and discussion

Synthesis of γ-turn analogues

We used a four step route employing a ring closing metathesis (RCM) procedure, analogous to that used by Hanessian and Angiolini in their preparation of β-turn mimetics (Scheme 1).[19] Initially, *N*-Boc-protected L-amino acids (**1** and **6**) were coupled with the methyl ester of L-allylglycine by the EDAC–HOBt–NEt_3 coupling procedure to give *N*-Boc-L-AA-L-allylglycine-OMe (**2** and **7**) (AA = amino acid residue; EDAC = 1-ethyl-3-(3-dimethylaminopropyl)carbodiimide hydrochloride; HOBT = 1-hydroxybenzotriazole hydrate). Deprotection of the *N*-Boc group of the dipeptide afforded the free amines, which were coupled with *N*-Boc-L-allylglycine to yield the substrates (**3** and **8**) for the RCM reaction. The precursors (**3** and **8**) underwent successful RCM using benzylidene[1,3-bis(2,4,6-trimethylphenyl)-2-imidazolidinylidene] dichloro (tricyclohexylphosphine) ruthenium[20] as catalyst to yield **4a** and **9**, respectively, as a mixture of *E*- and *Z*-isomers, in moderate to good yields. The *E*- and *Z*-isomers derived from the proline-containing peptide (**9**) were difficult to separate by chromatography and were thus used as a mixture in the hydrogenation step. In contrast, the corresponding *E*- and *Z*-isomers derived from **4a** were separable by chromatography. The targets ***E*-4b**, ***Z*-4b**, **5** and **10** were prepared from **4a** and **9** by hydrogenation and/or deprotection by saponification (LiOH–THF–H_2O) and CF_3CO_2H treatment. NMR analyses, predominantly in the form of NOEs, and molecular dynamics calculations were then used to investigate the solution conformations of the proposed γ-turn mimics ***E*-4b**, ***Z*-4b**, **5** and **10**.

Conformational studies of the γ-turn analogues

(*S*,*S*)-(7*Z*)-10-Amino-3,11-dioxo-1,4-diaza-cycloundec-7-ene-5-carboxylic acid (*Z*-4b). The ^{1}H NMR spectrum of ***Z*-4b** in $[^2H]_6$-DMSO at 298 K indicated the presence of two conformational isomers, A and B, in a 2 : 1 ratio, respectively, that were shown by 2D ROESY spectra to be undergoing exchange. In order to investigate the structures of the two conformers, further NMR analyses were carried out at low temperature in $[^2H]_5$-pyridine, which was the only solvent tested in which ***Z*-4b** was sufficiently soluble at low temperature. At 238 K, two ***Z*-4b** conformers A and B were present in a ratio of 2 : 1 as before. A full assignment and conformational study was performed at 238 K using standard 2D NMR techniques (see Experimental Section and ESI†). The temperature dependence of the amide proton chemical shifts was investigated between 278 and 233 K to investigate intramolecular hydrogen-bonding; the results revealed that the temperature dependence of the two ***Z*-4b** conformers was very similar and linear over this range. However, for both ***Z*-4b** conformers, the temperature coefficients of NH1 and NH4 differed significantly (−9.0 (A), −8.5 (B) ppb/K for NH1 and −5.0 (A), −4.5 (B) ppb/K for NH4). The NH temperature dependencies for NH1 *versus* NH4 suggests that in $[^2H]_5$-pyridine, a hydrogen-bonding solvent, NH4 has a greater propensity than NH1 for hydrogen-bonding in both ***Z*-4b** A and B, although the magnitude of the temperature coefficient suggests a rather weak hydrogen bond interaction.[21]

A more detailed analysis of the conformations was then undertaken through consideration of NOEs and spin coupling constants. At 238 K, conformational exchange between ***Z*-4b** conformers A and B was not observed on the NMR timescale, as shown by the loss of exchange cross peaks in the ROESY spectrum allowing a separation of the NOE data for each conformer (see ESI†). These data indicate that a principle difference between the ***Z*-4b** A and B conformers resides in the relative orientation of the alkene with respect to NH1 and NH4 (Fig. 2 and 3).

In ***Z*-4b** conformer A, strong NOEs between NH1 and H8, H5 and H7 and NH4 and H6 were observed; these imply that the alkene is on the same face as NH1 and H5, but on the opposite face to NH4. NOEs between NH1 and H10 and between H10 and H8 were also observed. A conformation consistent with all the available experimental data for ***Z*-4b** conformer A is shown in Fig. 2. The observed proton coupling constants provided

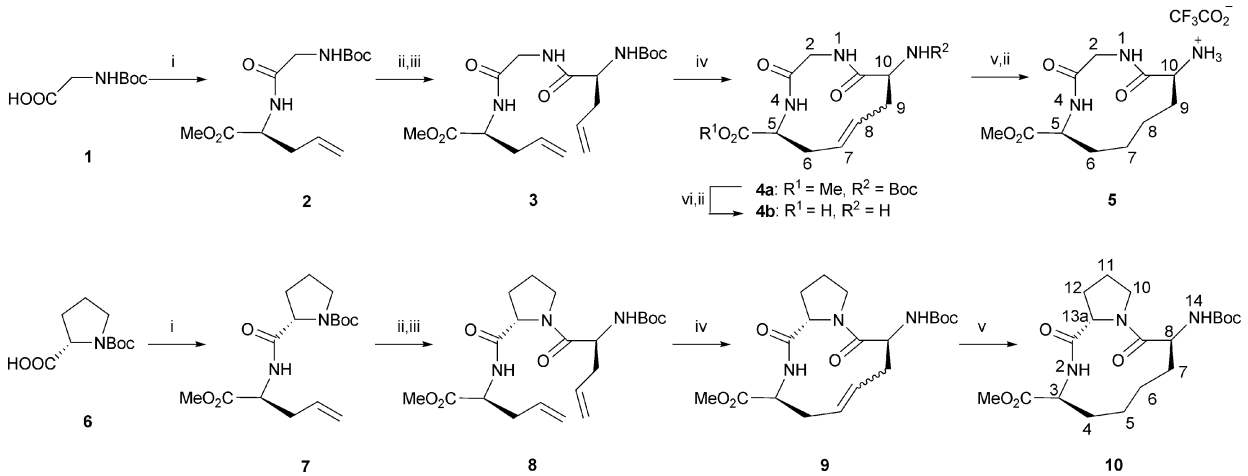

Scheme 1 *Reagents and conditions*: (i) EDAC, HOBt, NEt_3, L-allylgly-OMe·HCl, CH_3CN, 0 °C to rt., 6 h; (ii) CF_3CO_2H, CH_2Cl_2, 0 °C to rt., 30 min; (iii) EDAC, HOBt, NEt_3, *N*-Boc-L-allylgly-OH, CH_3CN, 0 °C to rt., 6 h; (iv) 10 mol% $(PCy_3)_2Cl_2Ru$ benzylidene catalyst, CH_2Cl_2, reflux, 8 h; (v) Pd/C, H_2, CH_2Cl_2; (vi) LiOH, THF, H_2O.

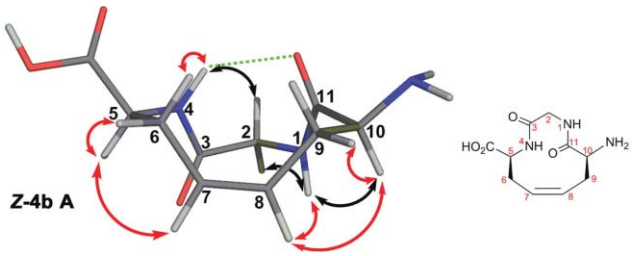

Fig. 2 View from a molecular model of ***Z*-4b** conformer A with significant NOEs indicated. NOEs shown in black are common to both ***Z*-4b** conformers A and B whereas those in red were characteristic of ***Z*-4b** conformer A.

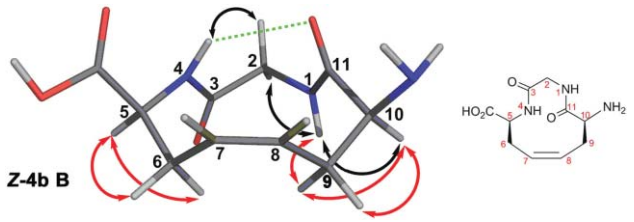

Fig. 3 View from a molecular model of ***Z*-4b** conformer B with significant NOEs indicated. NOEs shown in black are common to ***Z*-4b** both conformers A and B whereas those in red were characteristic of ***Z*-4b** conformer B.

further support for a well defined conformational preference (Table 1). The large coupling constants $^{3}J_{(NH4,H5)}$ (10.8 Hz), $^{3}J_{(H5,H6)}$ (11.0 Hz), and $^{3}J_{(H9,H10)}$ (12.6 Hz) were consistent with approximately antiperiplanar relationships between these protons. The calculated dihedral angles[22] showed good correspondence with those observed in the representative structure shown in Fig. 2. Together these observations indicate that the conformation of the eleven-membered ring of ***Z*-4b** conformer A adopts a '*chair–chair*' like structure, following the nomenclature employed by Katzenellenbogen *et al.* for 10-membered cyclic lactams.[23] In the chair–chair conformation, the protons on positions 5, 6, 9 and 10 of ***Z*-4b** conformer A may be described as occupying either *pseudo*-axial or *pseudo*-equatorial positions and hence both H5 and H10 may be considered to occupy *pseudo*-axial positions in the respective chairs.

In ***Z*-4b** conformer B, NOEs between NH1–H9′ and between NH1–H10, together with the absence of NH1–H8 and NH4–H6 NOEs (both observed strongly for ***Z*-4b** conformer A) defined the relative location of the alkene as being now away from NH1 and on the opposite face of the structure compared to the ***Z*-4b** conformer A (Fig. 3). Consistent with this change of orientation, NOEs of similar magnitude were observed between H10 and both H9 and H9′ as were NOEs between H5 and both H6 and H6′ for ***Z*-4b** conformer B. These data suggest H10 and H5 of ***Z*-4b** conformer B occupy *pseudo*-equatorial positions in the ring structure. The observed coupling constants concur, with the H10–H9/H9′ coupling constants both being small (<2 Hz), consistent with H10 bisecting the two H9 protons; the magnitude of the H5–H6/H6′ couplings could not be determined due to peak overlap (Table 1). Furthermore, NOEs between NH1–H2′ and NH4–H2 confirmed that the relative orientations of the amide groups were as in ***Z*-4b** conformer A. Together, these observations suggest that the alkene of ***Z*-4b** conformer B is on the same face as the carboxylic acid and free amine functionalities, in contrast to ***Z*-4b** conformer A. We propose that the ***Z*-4b** A–B interconversion arises from a series of torsional angle rotations of the single bonds between C5 and C10 allowed by the 11-membered ring, whilst the amide bonds remain *trans* and oriented in opposite directions.

For both ***Z*-4b** conformers A and B, it therefore appears that the 11-membered cyclic structure imposes an inverse γ-turn conformation centred about the glycine residue. The relevant ϕ and ψ angles for the proposed structures fall within the definitions of an inverse γ-turn ($\phi = -79 \pm 40°$, $\psi = 69 \pm 40°$) (Table 2).[6,24] It is clear, however, that the geometry of the hydrogen bond of the γ-turn is likely distorted with the H-bond angles indicating rather poor linearity, as is apparent in the proposed structures (Fig. 2 and 3). This may be a consequence of the highly constrained cyclic structures rendering it not possible for the NH4 and C11=O groups to readily approach co-planarity. Such geometrical constraints also appear to limit the conformational flexibility of ***Z*-4b** conformers and allow only a slow "flip–flop" interchange between the A and B conformers by rotational inversion of the alkene linker.

(*S*,*S*)-(7*E*)-10-Amino-3,11-dioxo-1,4-diaza-cycloundec-7-ene-5-carboxylic acid (*E*-4b). The proton spectrum of the *E*-unsaturated glycine derived ***E*-4b** at room temperature displayed broad exchanging signals which could not be adequately assigned using two-dimensional NMR experiments. The low temperature proton spectrum in [^{2}H]$_5$-pyridine (238 K) revealed four ***E*-4b** conformers A, B, C, and D in a ratio of ~1 : 1 : 0.1 : 0.02.

Table 1 Observed ^{3}J-coupling constants, calculated dihedral angles and dihedral angles from energy minimised structures for ***Z*-4b** conformers A and B

	***Z*-4b** Conformer A			***Z*-4b** Conformer B		
	$(^{3}J_{H,H})$/Hz	$\theta°$ $(^{3}J_{H,H})^{a}$	$\lvert\theta°\rvert$ (model)	$(^{3}J_{H,H})$/Hz	$\theta°$ $(^{3}J_{H,H})^{a}$	$\lvert\theta°\rvert$ (model)
H10–H9	12.6	161	180	<2	>69	55
H10–H9′	3.1	61	64	<2	>69	61
NH4–H5	10.8	180	172	9.6	173	159
NH1–H2′	8.0	151	168	9.3	166	168
NH1–H2′	3.8	48	47	3.7	50	46
H5–H6	11.0	168	176	—[b]	—	—
H5–H6′	2.6	70	61	—[b]	—	—

[a] Calculated dihedral angles θ $(^{3}J_{H,H})$ were obtained from equation $^{3}J_{NH\alpha} = 6.4\cos^{2}\theta - 1.4\cos\theta + 1.9$.[22] [b] J values could not be measured due to peak overlap for H5, H6 and H6.

Table 2 Dihedral angles of inverse γ-turn analogues (defined by NMR and molecular modelling) compared to those from the $HIF_{802-804}$ crystal structure[8]

	Dihedral angles/°		*N*H–*O*=C	N*H*–O=*C*	N*H*–*O*=C
	ϕ	ψ	Angle/°	Angle/°	Distance/Å
***Z*-4b** Conformer A	−80	79	135	101	2.1
***Z*-4b** Conformer B	−83	79	136	98	2.2
***E*-4b** Conformer A	−82	52	145	88	2.0
***E*-4b** Conformer B	−81	62	142	95	2.0
5 Conformer A	−83	50	146	84	2.1
10	−76	62	136	99	2.0
$HIF_{802-804}$[8]	−78	61	147	102	1.9

The assignments of the proton spectra for three of the ***E*-4b** conformers A, B, and C could be achieved using standard 2D NMR techniques (see ESI† Tables 1–3); ***E*-4b** conformer D was too low in concentration to be assigned. Even at 238 K, ***E*-4b** conformers A and B still underwent exchange on the NMR timescale, and the NH signals were too broad to decipher structurally relevant coupling constants (the only discernable NH coupling constant was that of NH4 for the ***E*-4b** minor conformer C, $^3J_{(NH4,H5)} = 8$ Hz).

The exchange processes at 238 K for ***E*-4b** apparently involved two pairs of ***E*-4b** conformers: (i) A with B, and (ii) C with D. Evidence for these pairs came from exchange mediated NOE crosspeaks in the 2D ROESY spectra where no A–B to C–D exchange was detected. The significant exchange averaging of the NOEs observed for ***E*-4b** conformers A and B precluded the semi-quantitative analysis of NOE intensities. Hence a qualitative interpretation of the data, combined with comparisons with those obtained for the conformers of ***Z*-4b**, was employed to investigate the ***E*-4b** A–B exchange processes. It became apparent that the relationship between the two amide groups of ***E*-4b** was as observed for ***Z*-4b**; a consistent set of NOEs between NH1, glycine H2/H2′ and NH4 defined this relationship, with no other NOEs present to contradict this geometry. Given this constraint, and the geometry imposed by the *E*-alkene, there is very limited available torsional flexibility to enable conformational interchange between ***E*-4b** A and B; we propose that the only readily achievable exchange process arises from rotational inversion of the alkene (Fig. 4). The observed NOE patterns (notably those involving NH4, H6/H6′ and H8; see ESI†) supported the existence of the ***E*-4b** A and B conformers, although it was not possible to reliably define assignments for each because of the exchange averaging of the NOE data. In the ***E*-4b** A and B conformers the inversion of the alkene geometry would probably be a facile process relative to that of ***Z*-4b** involving, primarily, rotation about the C6–C7 and C8–C9 bonds, consistent with the observed conformational exchange between ***E*-4b** A and B at 238 K. The similar populations of conformers A and B of ***E*-4b** indicate there was no preference for either form, consistent with their structural similarities.

In contrast, ***E*-4b** conformer C showed no evidence for exchange with ***E*-4b** conformers A and B at 238 K, but did exchange with the ***E*-4b** minor conformer D at this temperature. Attempts to observe exchange of conformer C with ***E*-4b** conformers A or B by recording data at higher temperatures led to highly overlapped, broad and complex spectra that could not be interpreted further. The observed NOEs for ***E*-4b** conformer C differed somewhat from those of ***E*-4b** A and B and most strikingly presented a clear NH1–NH4 NOE. This observation, together with the accompanying NH1–H10 NOE, suggests that the C3–N4 amide bond has inverted (whilst retaining its *trans* geometry) such that the two amide NH protons are now on the same face as one another (Fig. 5), in contrast to the previously described conformations. The available data were insufficient to define reliably the orientation of the alkene in ***E*-4b** conformer C and an arbitrary representation is given in Fig. 5. Although we lack conclusive evidence due to the very low levels of ***E*-4b** conformer D and the spectral complexity present, it would seem reasonable to suppose ***E*-4b** conformer D arises from inversion of the alkene orientation relative to ***E*-4b** conformer C, as for the ***Z*-4b** and ***E*-4b** conformer A–B interchanges. We propose that the inversion of the ***E*-4b** C3–N4

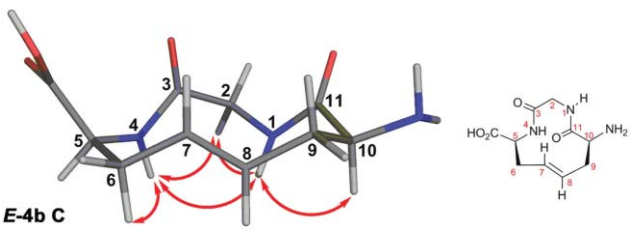

Fig. 5 View from a molecular model of compound ***E*-4b** conformer C. Significant NOEs are indicated although insufficient data were available to define the alkene orientation and an arbitrary C7-up, C8-down relationship is shown.

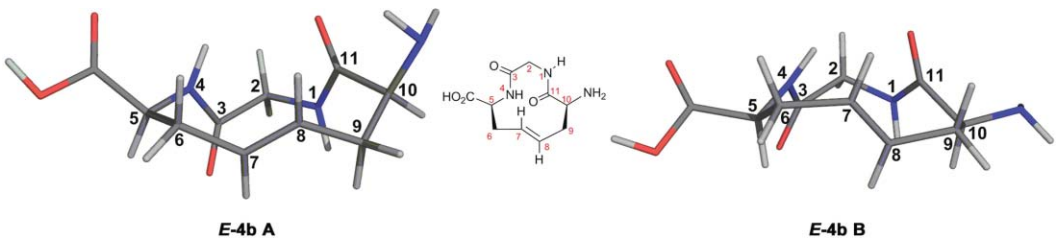

Fig. 4 View from a molecular model of ***E*-4b** showing the two conformational forms related by inversion of the alkene geometry.

amide occurs at a slower rate than the alkene inversion and hence the ***E*-4b** A–B-C–D exchange was not detected at 238 K. Again, as for ***Z*-4b**, ***E*-4b** conformers A and B may be considered inverse γ-turn analogues whereas ***E*-4b** conformer C does not match this geometry.

(5*S*,10*S*)-10-Amino-3,11-dioxo-1,4-diazacycloundecane-5-carboxylic acid (5). The saturated glycine-containing analogue **5** also demonstrated the presence of multiple conformers at room temperature in both pyridine and chloroform. Analyses carried out in $[^2H]_5$-pyridine at 238 K revealed the presence of two conformers A and B of **5** in a 3 : 1 ratio (see ESI†).

Conformers A and B of **5** were characterised by analyses of their NOE data observed in ROESY spectra at 238 K. For both conformers **5** A and B, no NH1–NH4 NOE was observed indicating these NH protons reside on opposite faces of the ring, as previously defined for the major conformers of ***Z*-4b** and ***E*-4b**. Both **5** A and B displayed a strong NH1–H10 NOE indicative of a *trans*-N1–C11 amide bond geometry. For **5** conformer A the pattern of NOEs involving NH1, H2/H2′ and NH4 indicated a relative geometry of the amide groups as seen previously in ***Z*-4b** A and B and ***E*-4b** A and B (Fig. 6), whereas the NOEs involving the C5–C10 linker of **5** conformer A did not match well with any single conformation and it seems likely that this region of the molecule is flexible and is able to undergo conformational averaging. Strong NOEs were observed between the H5 and both H6 protons, and H10 displayed NOEs to both H9 protons. Weaker NOEs were observed between the NH1 and H8 and H9 protons which may arise from greater flexibility of the C6–C9 region. Overall, the major conformer A of **5** appears to adopt the inverse γ-turn but retains greater internal flexibility of its linker region than that seen for the alkene analogues.

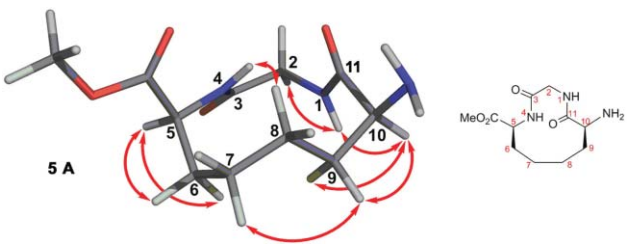

Fig. 6 View from a molecular model of **5** conformer A showing the inverse γ-turn orientation. NOE data suggest conformational flexibility remains in the saturated linker.

The data for **5** conformer B suggests different behaviour of the C3–N4 amide functionality, evidence for which comes from the unique and intense NH1–H5 NOE as well as the unusually weak NOEs from NH4 to both H2 protons. The close proximity of NH1 to both H5 and H10 requires the C3–N4 amide bond to occupy a *cis*-geometry (Fig. 7), probably achieved most readily from **5** conformer A by inversion of the C3 amide carbonyl group.

(3*S*,8*S*,13*aS*)-Methyl 8-(tert-butoxycarbonylamino)-1,9-dioxo-dodecahydro-1*H*-pyrrolo[1,2-*a*][1,4]diazacycloundecine-3-carboxylate (10). The *N*-Boc-protected saturated proline-containing cyclic analogue (**10**) was analysed in $CDCl_3$ at 298 K. Uniquely, when compared to the glycine analogues (***Z*-4b**, ***E*-4b** and **5**) analysed here, the data indicated the presence of only a single and well-resolved set of resonances (see ESI†). The amide temperature

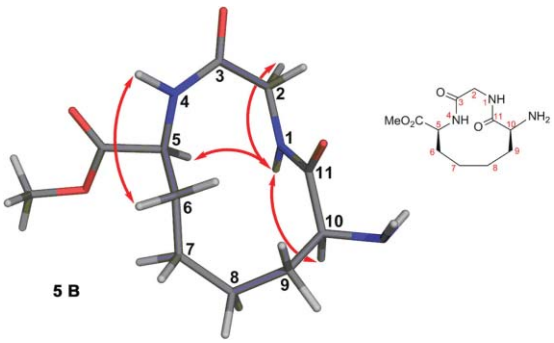

Fig. 7 View from a molecular model of **5** conformer B showing the C3–N4 *cis*-amide and the relevant NOEs that define the conformation.

coefficient ($\Delta\delta/\Delta T$) of NH2 of **10** was found to be only −0.9 ppb/K and the proton shift was largely insensitive to the addition of DMSO (Fig. 8). As the proton was significantly invariant to these changes and displayed a chemical shift value (7.3 ppm) intermediate between that expected for an amide proton participating in a strong H-bond (> 7.5 ppm) and that in the free state (< 7 ppm), these data suggest some involvement in intramolecular hydrogen bonding. In contrast, NH14 displayed acute sensitivity to DMSO addition suggesting this amide NH to be relatively exposed.

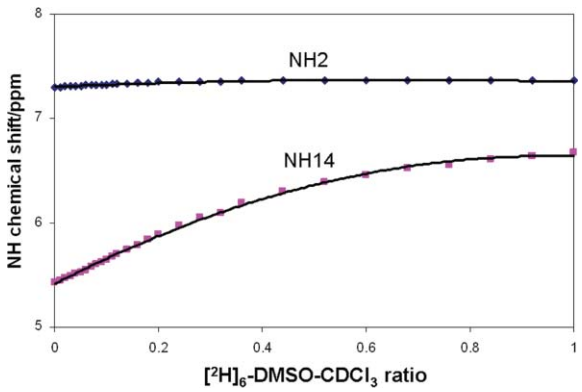

Fig. 8 $[^2H]_6$-DMSO titration of **10** in $CDCl_3$.

The NOEs observed in a 2D NOESY experiment with **10** were again consistent with an inverse γ-turn geometry (Fig. 9, and ESI†) but showed evidence for flexibility within the saturated linker once again, including NOEs from H10 on the proline C^δ to protons along the linker from H8 across to H5. A molecular dynamics simulation with **10** showed there to be little flexibility within the γ-turn region but that significant mobility was present in the linker region and, as expected, in the unconstrained ester and Boc groups (Fig. 10). The absence of a second conformer for **10** presumably arises because of the additional constraints imposed by the proline ring. Indeed, modelling suggests that the presence of either a *cis*-amide at C1–N2 or a *cis*-proline amide would lead to considerable steric interaction between the proline ring and linker protons.

From these data, we propose the proline-containing cyclic analogue **10** adopts a similar inverse γ-turn motif to that observed for the major conformers of the other cyclic analogues presented in Table 2, in which there is a weak hydrogen-bond association forming a seven-membered ring. In other proline containing peptides, there is also a strong propensity to form inverse γ-turns

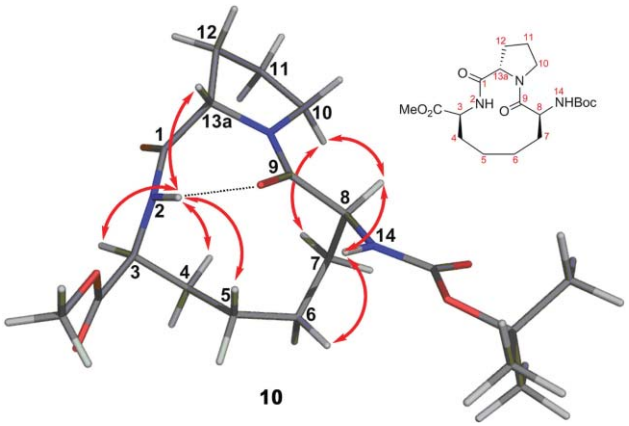

Fig. 9 Representative conformer of **10** showing significant NOE correlations and a partial intramolecular hydrogen bond contact between NH2 and C9=O.

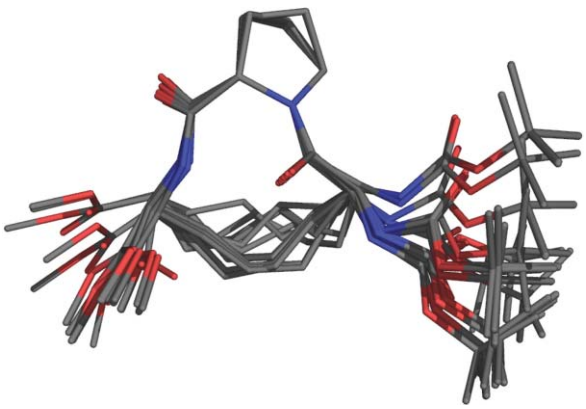

Fig. 10 Superimposed ensemble of energy minimised conformers of **10** generated from a molecular dynamics simulation showing the proposed inverse γ-turn and flexibility of the alkyl linker moiety.

where proline is the (*i*+1)th residue of the turn.[25–27] This occurs even in open chain natural products, such as proctolin (Arg-Tyr-Leu-Pro-Thr), which contains a hydrogen bond between Thr NH and Leu CO and a salt bridge between its N- and C-termini.[28]

Conclusions

The results of the combined synthetic and spectroscopic analyses described here suggest that it is possible to prepare monocyclic analogues that constrain peptidomimetics in conformations closely analogous to inverse γ-turns. Our work has focused on peptidomimetics of the Val-Asn-Ala fragment of hypoxia inducible factor-1α (HIF-1α) that forms an inverse γ-turn as observed in an X-ray structure of a HIF-1α fragment bound to FIH (factor inhibiting HIF). During our studies it became apparent that the synthetic cyclic peptide analogues displayed a structural propensity to form inverse γ-turn conformations probably due to restricted conformational mobility associated with torsional rotation of the linker fragment. This proposed formation of γ-turn type structures was supported by extensive NMR analyses.

For the analogues containing the unsaturated linkers (***Z*-4b** and ***E*-4b**), there was clear evidence for two dominant conformational forms in which the alkene orientation could switch between "up" and "down" states. Substituting a *trans*- for a *cis*-alkene in the linker led to a more conformationally labile exchange process. In the glycine-derived saturated analogue **5**, we observed increased flexibility in the saturated system as a whole as noted by the identification of two conformers (3 : 1 ratio) in which the predominant one contains an inverse γ-turn, whereas the minor conformer does not, but instead uniquely displays a *cis*-amide bond. The proline saturated peptide **10** again contained a stable inverse γ-turn involving folding of the alkyl chain towards the proline ring but displayed no evidence of slow conformational interconversion. The combined results reveal that it should be possible to tune the overall conformation(s) of the analogues and their flexibility by appropriate modification of the linker.

When compared to the γ-turn identified in the crystal strucutre of HIF-1α–FIH complex, it appears that some of the analogues can adopt conformations that closely match that of the $HIF_{802–804}$ residues at the FIH active sites (Table 2 and Fig. 11). Future work will be directed towards elaborating the core γ-turn analogues in order to bind to FIH and investigation of these variants as inhibitors and probes for conformational changes in FIH catalysis. Developments of the analogues reported here, *e.g.* by incorporation into ankyrin repeat domain proteins,[14] may provide insights into the mechanism by which these proteins bind to FIH.

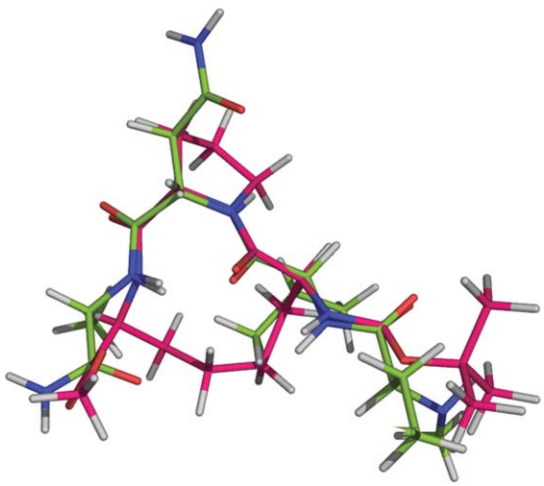

Fig. 11 Superposition of a predicted conformation of γ-turn analogue **10** (pink) and the conformation that a fragment of HIF-1α adopts at the active site of FIH (green).[8]

Experimental section

Materials and methods

Reagents and solvents were from commercial sources unless otherwise stated. Flash chromatography was performed using silica gel (0.125–0.25 mm, 60–120 mesh) as the stationary phase. Thin layer chromatography (TLC) was performed on aluminium plates pre-coated with silica gel (Merck silica gel 60 F_{254} 1.05554), which were visualised by the quenching of UV fluorescence (using an irradiation wavelength λ_{max} 254 nm), and/or by staining with

iodine or anisaldehyde in solution, followed by heating. Proton magnetic resonance spectra (^{1}H NMR) were recorded on Bruker AV400 (400 MHz), Bruker DRX500 (500 MHz), and Bruker AV500 (500 MHz) spectrometers at ambient temperature. Carbon magnetic resonance spectra (^{13}C NMR) were recorded on Bruker DPX400 (100 MHz), Bruker AV400 (100 MHz), Bruker DRX500 (125 MHz), and Bruker AV500 (125 MHz) spectrometers at ambient temperature. Chemical shifts (δ_H and δ_C) are quoted in parts per million (ppm) and are referenced to the residual solvent peak; coupling constants (J) are quoted in Hertz (Hz) to the nearest 0.5 Hz. The following abbreviations are used: br, broad singlet; s, singlet; d, doublet; t, triplet; q, quartet; dd, doublet of doublets; m, multiplet. High-resolution mass spectra were recorded on a VG Autospec spectrometer by chemical ionisation or on a Micromass LCT electrospray ionisation mass spectrometer operating at a resolution of 5000 full width half height. Melting points (mp) were recorded using a Leica Galen III microscope. Infrared absorption spectra were recorded using a Nicolet 210 FT-IR absorption spectrometer.

(*S*)-Methyl 2-(2-(*tert*-butoxycarbonylamino)acetamido)pent-4-enoate or *N*-Boc-Gly-L-allylglycine-OMe (2). To a stirred solution of *N*-Boc-Gly-OH (1.14 g, 6.52 mmol), EDAC (1.87 g, 9.8 mmol), HOBt (1.32 g, 9.8 mmol) and triethylamine (1.37 mL, 9.8 mmol) in CH_3CN (20 mL) at 0 °C under a nitrogen atmosphere was added a solution of L-allylglycine methyl ester hydrochloride salt (1.08 g, 6.52 mmol) in CH_3CN (15 mL). The mixture was allowed to warm to room temperature and stirred for 6 hours, and then quenched with a saturated $NaHCO_3$ solution (20 mL). The reaction mixture was then extracted with EtOAC (3 × 50 mL). The organic layers were washed with brine and dried over Na_2SO_4. Following filtration, the solvent was evaporated to give a residue which was purified by flash column chromatography (EtOAc–petroleum spirit, 3 : 7) to give **2** (1.36 g, 73%). **2**: colourless gum; FT-IR (KBr) 3322 (br), 2979, 1681, 1522 cm^{-1}; δ_H (400 MHz, $CDCl_3$): 6.59 (d, J = 7.1 Hz, 1H, NH1′), 5.73–5.62 (m, 1H, H4), 5.16 (s, 1H, NH4′), 5.13–5.11 (m, 2H, 2 × H5), 4.72–4.67 (m, 1H, H2), 3.90–3.80 (m, 2H, 2 × H3′), 3.76 (s, 3H, OMe), 2.62–2.51 (m, 2H, 2 × H3), 1.47 (s, 9H, $C(CH_3)_3$); δ_C (100 MHz, $CDCl_3$): 171.9, 169.1, 155.3, 131.8, 119.5, 80.5, 52.5, 51.5, 43.2, 36.4, 28.2; HRMS calcd. for $C_{13}H_{22}N_2O_5$ $[M - H]^-$ 285.1450, found 285.1456.

(6*S*,12*S*)-Methyl 6,12-diallyl-2,2-dimethyl-4,7,10-trioxo-3-oxa-5,8,11-triazatridecan-13-oate or *N*-Boc-L-allylglycine-glycine-L-allylglycine-OMe (3). To a stirred solution of **2** (1.36 g, 4.74 mmol) in CH_2Cl_2 (20 mL) at 0 °C under a nitrogen atmosphere was added CF_3CO_2H (4 mL). The reaction mixture was then stirred at room temperature under a nitrogen atmosphere for 2 hours. The solvent and CF_3CO_2H were then evaporated to give a pale yellow liquid, which was dissolved in CH_3CN (10 mL). The mixture was added to a solution of *N*-*tert*-butoxycarbonyl-L-allylglycine (1.02 g, 4.74 mmol), EDAC (1.36 g, 7.11 mmol), HOBt (960 mg, 7.11 mmol) and triethylamine (1 mL, 7.11 mmol) in CH_3CN (15 mL) at 0 °C under a nitrogen atmosphere. The reaction mixture was stirred at room temperature for 6 hours, then quenched with a saturated $NaHCO_3$ solution (20 mL), then extracted with EtOAc (3 × 30 mL). The combined organic layers were washed with brine and dried over sodium sulfate. Following filtration, the solvent was evaporated to give a residue, which was further purified by flash column chromatography (EtOAc–petroleum spirit, 1 : 1) to give **3** (1.24 g, 64%). **3**: colourless gum; FT-IR (film) 3309, 3079, 2980, 1661, 1530 cm^{-1}; δ_H (400 MHz, $CDCl_3$): 7.28 (s, 1H, NH8), 7.18 (s, 1H, NH11), 5.76–5.64 (m, 2H, 2 × $CHCH_2CHCH_2$), 5.30 (s, 1H, NH5), 5.14–5.06 (m, 4H, 2 × $CHCH_2CHCH_2$), 4.65–4.59 (m, 1H, H12), 4.21–4.20 (m, 1H, H6), 4.04 (dd, J = 16, 5.5 Hz, 1H, H7), 3.91 (dd, J = 16, 5.5 Hz, 1H, H7′), 3.70 (s, 3H, OMe), 2.57–2.42 (m, 4H, 2 × $CHCH_2CHCH_2$), 1.40 (s, 9H, $C(CH_3)_3$); δ_C (100 MHz, $CDCl_3$): 172.2, 171.9, 168.7, 155.6, 133.0, 132.1, 119.1, 119.0, 80.1, 53.9, 52.3, 51.9, 43.0, 36.8, 36.2, 28.2; HRMS calcd. for $C_{18}H_{29}N_3O_6$ $[M + H]^+$ 384.2134, found 384.2066.

(5*S*,10*S*)-Methyl 10-(*tert*-butoxycarbonylamino)-3,11-dioxo-1,4-diazacycloundec-7-ene-5-carboxylate (4a). To a light purple solution of Grubbs' ruthenium benzylidene catalyst (78.5 mg, 0.092 mmol) in 1 L anhydrous CH_2Cl_2 under a nitrogen atmosphere was added a solution of **3** (708 mg, 1.85 mmol) in anhydrous CH_2Cl_2 (50 mL) *via* a cannula; the purple colour immediately faded to yellow. The reaction mixture was refluxed for 8 hours, then quenched by the addition of water (1 mL) and the solvent was removed under vacuum to afford a black residue, which was directly loaded onto a chromatography column (EtOAc–petroleum spirit, 7 : 3) to afford compounds ***Z*-4a** (203.5 mg, 31%) and ***E*-4a** (256.1 mg, 39%).

***Z*-4a.** White solid; mp 137–139 °C; $[\alpha]_D^{20}$ −104.5 (c = 0.5 in CH_2Cl_2); FT-IR (KBr) 3305, 2977, 1764, 1697, 1647, 1530 cm^{-1}; δ_H (500 MHz, $CDCl_3$): the spectrum was complex due to the presence of the conformational isomers with up to two signals for each hydrogen. 7.10 (s, *ca.* 0.3H, NH1B), 6.83 (s, *ca.* 0.7H, NH1A), 6.60 (d, J = 11 Hz, *ca.* 0.7H, NH4A), 6.55 (d, J = 10 Hz, *ca.* 0.3H, NH4B), 5.70–5.20 (m, 3H, H7, H8 and N*H*Boc), 4.83–4.81 (m, *ca.* 0.3H, H5B), 4.58–4.45 (m, 2H, H5A, H10B and H2/H2′), 4.13–4.02 (m, *ca.* 0.7H, H10A), 3.71–3.69 (m, 3H, OMe), 3.22–3.13 (m, 1H, H2′/H2), 2.49–2.44 (m, 4H, H6, H6′, H9 and H9′), 1.38–1.36 (m, 9H, $C(CH_3)_3$); δ_C (125 MHz, $CDCl_3$): 174.6, 172.7, 171.5, 170.8, 170.4, 169.2, 155.3, 155.2, 129.0, 128.8, 127.9, 127.7, 80.5, 80.3, 54.0, 52.6, 51.8, 50.8, 45.0, 44.8, 43.0, 33.2, 32.6, 31.3, 30.1, 30.0, 28.4, 28.3; HRMS calcd. for $C_{16}H_{25}N_3O_6$ $[M - H]^-$ 354.1665, found 354.1664.

***E*-4a.** White solid; mp 141–145 °C; $[\alpha]_D^{20}$ −104.0 (c = 0.5 in CH_2Cl_2); FT-IR (KBr) 3345, 2979, 1673, 1530 cm^{-1}; δ_H (500 MHz, $[^2H]_6$-DMSO, 363 K): 8.03 (br, 1H, NH1), 6.96 (d, J = 5 Hz, 1H, NH4), 6.74 (br, 1H, N*H*Boc), 5.18–5.08 (m, 1H, H8), 5.10–5.00 (m, 1H, H7), 4.37–4.29 (m, 1H, H5), 4.12–4.04 (m, 1H, H10), 3.75–3.65 (m, 4H, OMe and H2), 3.64–3.54 (m, 1H, H2′), 2.65–2.56 (m, 1H, H6), 2.50–2.40 (m, 1H, H9), 2.30–2.22 (m, 1H, H9′), 2.22–2.10 (m, 1H, H6′), 1.41 (s, 9H, $C(CH_3)_3$); δ_C (125 MHz, $[^2H]_6$-DMSO, 363 K): 172.5, 172.4, 170.1, 155.4, 130.4, 128.8, 79.2, 56.0, 52.4, 50.5, 44.8, 36.0, 35.7, 28.7; HRMS calcd. for $C_{16}H_{25}N_3O_6$ $[M - H]^-$ 354.1665, found 354.1667.

(5*S*,10*S*)-10-Amino-3,11-dioxo-1,4-diazacycloundec-7-ene-5-carboxylic acid (*Z*-4b). To a stirred solution of ***Z*-4a** (60.7 mg, 0.17 mmol) in THF and H_2O (4 : 1, 2.5 mL) at 0 °C was added LiOH (6.2 mg, 0.26 mmol). The reaction mixture was slowly warmed to room temperature and stirred for 2 hours. After the disappearance of starting material as observed by TLC analysis, the reaction mixture was diluted (5 mL H_2O) and washed with EtOAc (2 × 5 mL). The aqueous layer was acidified with saturated

citric acid aqueous solution to pH 2 and extracted with EtOAc (3 × 10 mL). The combined organic layers were dried over sodium sulfate, filtered, and concentrated to afford a clear film. After drying overnight under vacuum, the film was dissolved in CH_2Cl_2 (1 mL) and CF_3CO_2H (1 mL) was added under a nitrogen atmosphere. The reaction mixture was stirred for 2 hours and then concentrated to obtain ***Z*-4b** (38.3 mg, 93%). ***Z*-4b**: white solid; mp 145–146 °C; FT-IR (KBr) 3365, 1680, 1540, 1435 cm^{-1}; δ_H (500 MHz, $[^2H]_5$-pyridine, 238 K): 11.32–11.27 (m, *ca.* 0.7H, NH1A), 11.07–11.04 (m, *ca.* 0.3H, NH1B), 7.63 (d, $J = 9.6$ Hz, *ca.* 0.3H, NH4B), 7.60 (d, $J = 10.8$ Hz, *ca.* 0.7H, NH4A), 6.30–6.15 (m, *ca.* 0.3H, H8B), 5.70–5.59 (m, 1H, H7A and H7B), 5.46–5.36 (m, 1H, H5B and H8A), 5.35–5.31 (m, *ca.* 0.3H, H10B), 5.25–5.17 (m, *ca.* 0.7H, H5A), 4.94–4.84 (m, 1H, H10A and H2B), 4.80–4.73 (dd, $J = 13.0$, 8.0 Hz, *ca.* 0.7H, H2A), 3.57–3.51 (m, *ca.* 0.3H, H2′B), 3.44–3.8 (dd, $J = 13.0$, 3.7 Hz, *ca.* 0.7H, H2′A), 3.18–2.90 (m, 2H, H9A, H9′A, H9B and H9′B), 2.74–2.56 (m, 2H, H6A, H6′A, H6B and H6′B); HRMS calcd. for $C_{10}H_{15}N_3O_4$ $[M - H]^-$ 240.0984, found 240.0983.

(5*S*,10*S*)-10-Amino-3,11-dioxo-1,4-diazacycloundec-7-ene-5-carboxylic acid (*E*-4b). The synthesis of ***E*-4b** was carried out from ***E*-4a** in a manner analogous to that used for the preparation of compound ***Z*-4b** by hydrolysis of ***E*-4a** (19.9 mg, 0.056 mmol) and *N*-Boc-deprotection to afford ***E*-4b** (11.6 mg, 61%). ***E*-4b**: white solid; mp > 205 °C; FT-IR (KBr) 3467, 2967, 1682, 1574, 1510 cm^{-1}; δ_H (500 MHz, $[^2H]_5$-pyridine, 238 K): 11.10 (br, *ca.* 0.1H, NH1C), 10.97 (br, 1H, NH1A), 10.66 (br, 1H, NH1B), 9.80 (br, *ca.* 0.1H, NH4C), 8.64 (br, 1H, NH4A), 7.90 (br, *ca.* 0.022H, NH4D), 7.60 (br, 1H, NH4B), 6.18–6.10 (m, *ca.* 0.1H, H8C), 5.85–5.70 (m, 1H, H8A), 5.46–5.35 (m, *ca.* 1.1H, H8B and H7C), 5.35–5.10 (m, *ca.* 4.1H, H5A, H7A, H7B, H10B and H10C), 4.95–4.56 (m, *ca.* 4.1H, H2A, H2B, H5B, H5C and H10A), 4.45–4.38 (m, *ca.* 0.1H, H2C), 3.83–3.75 (m, *ca.* 0.1H, H9C), 3.70–3.63 (m, *ca.* 0.1H, H2′C), 3.45–3.35 (m, 1H, H2′B), 3.32–3.23 (m, 1H, H2′A), 3.18–3.00 (m, 1H, H9A and H9B), 3.00–2.84 (m, *ca.* 0.2H, H6C and H9′C), 2.82–2.48 (m, *ca.* 2.1H, H6A, H6B, H9′A, H9′B, H6′C), 2.40–2.30 (m, 1H, H6′B), 2.15–2.04 (m, 1H, H6′A); HRMS calcd. for $C_{10}H_{15}N_3O_4$ $[M - H]^-$ 240.0984, found 240.0983.

(5*S*,10*S*)-Methyl 10-(*tert*-butoxycarbonylamino)-3,11-dioxo-1,4-diazacycloundecane-5-carboxylate (11). To a stirred solution of **4a** (151.7 mg, 0.427 mmol) in EtOAc (1 mL) was added 10% Pd/C (6.4 mg). The mixture was stirred vigorously at room temperature under a hydrogen atmosphere overnight. The mixture was filtered and the solvent was removed under reduced pressure to obtain compound **11** (132.2 mg, 87%). **11**: white solid; mp 172–173 °C; $[\alpha]_D^{20}$ −74.9 (*c* 0.25 in CH_2Cl_2); FT-IR (film) 3323, 2953, 1674, 1520 cm^{-1}; δ_H (500 MHz, $CDCl_3$): 7.21 (br, 1H, NH1), 6.86 (d, $J = 8.5$ Hz, 1H, NH4), 5.47 (d, $J = 6.5$ Hz, 1H, N*H*Boc), 4.75–4.60 (m, 2H, H2 and H-5), 4.40–4.28 (m, 1H, H10), 3.80 (s, 3H, OMe), 3.33 (d, $J = 12.5$ Hz, 1H, H2′), 2.08–1.30 (m, 17H, H6, H6′, H7, H7′, H8, H8′, H9, H9′ and C(CH_3)$_3$); δ_C (125 MHz, $CDCl_3$): 175.2, 171.6, 169.8, 155.1, 80.0, 53.7, 52.6, 52.5, 45.5, 29.9, 28.4, 28.1, 22.9, 21.4; HRMS calcd. for $C_{16}H_{27}N_3O_6$ $[M - H]^-$ 356.1822, found 356.1836.

(5*S*,10*S*)-Methyl 10-amino-3,11-dioxo-1,4-diazacycloundecane-5-carboxylate (5). The Boc-deprotection of **11** was carried out to afford **5** (31.3 mg, 92%). **5**: white solid; mp > 220 °C; FT-IR (KBr) 3366, 3290, 2954, 1720, 1685, 1636 cm^{-1}; δ_H (500 MHz, $[^2H]_5$-pyridine, 238 K): 11.24 (br, *ca.* 0.3H, NH1B), 11.10 (dd, $J = 9.5$, 2.8 Hz, 1H, NH1A), 9.56 (d, $J = 11.5$ Hz, *ca.* 0.3H, NH4B), 8.33 (br, 1H, NH4A), 5.26 (td, $J = 11.5$, 2.5 Hz, *ca.* 0.3H, H2B), 5.08 (br, 1H, H10A), 5.00–4.84 (m, *ca.* 2.3H, H2A, H5A and H10B), 4.60–4.47 (m, *ca.* 0.6H, H2B and H2′B), 3.58–3.48 (m, 4H, H2′A and OMe), 2.66–2.56 (m, *ca.* 0.3H, H9B), 2.46–2.28 (m, 2H, H9A and H9′A), 2.00–1.89 (m, 1H, H6B), 1.88–1.52 (m, *ca.* 4.8H, H6B, H6′A, H6′B, H7B, H8A, H8B, H8′A, H8′B and H9′B), 1.50–1.40 (m, *ca.* 1.3H, H7A and H7′B), 1.18–1.05 (m, 1H, H7′A); HRMS calcd. for $C_{11}H_{19}N_3O_4$ $[M - H]^-$ 256.1298, found 256.1290.

(*S*)-*tert*-Butyl 2-((*S*)-1-methoxy-1-oxopent-4-en-2-ylcarbamoyl)-pyrrolidine-1-carboxylate (7). The synthesis of **7** was carried out in a manner analogous to that used for the preparation of compound **2** by coupling of *N*-Boc-L-Pro-OH (0.94 g, 4.3 mmol) with L-allylgly-OMe (0.72 g, 4.3 mmol), followed by column chromatography (EtOAc–petroleum spirit, 1 : 3) to yield the desired compound (**7**) (0.97 g, 68%). **7**: white solid; mp 72–74 °C; FT-IR (film) 3312, 2978, 1747, 1698, 1537, 1396, 1165 cm^{-1}; δ_H (500 MHz, $CDCl_3$): 7.38 (br, *ca.* 0.5H), 6.55 (br, *ca.* 0.5H), 5.69–5.63 (m, 1H), 5.11–5.07 (m, 2H), 4.66–4.63 (m, 1H), 4.32–4.24 (m, 1H), 3.74 (s, 3H), 3.50–3.28 (m, 2H), 2.62–2.55 (m, 1H), 2.51–2.44 (m, 1H), 2.32–1.87 (m, 1H), 1.95–1.80 (m, 3H), 1.46 (s, 9H); HRMS calcd. for $C_{16}H_{26}N_2O_5$ $[M + H]^+$ 327.1920, found 327.1916.

(*S*)-Methyl 2-((*S*)-1-((*S*)-2-(*tert*-butoxycarbonylamino)pent-4-enoyl)pyrrolidine-2-carboxamido)pent-4-enoate (8). The synthesis of **8** was carried out in a manner analogous to that used for the preparation of compound **3** by deprotection of **7** (948 mg, 2.9 mmol), coupling of the resultant amine with *N*-Boc-L-allylgly-OH (322 mg, 2.49 mmol), followed by column chromatography (EtOAc–petroleum spirit, 7 : 13) to yield **8** (936 mg, 76%). **8**: colourless gum; FT-IR (film) 3309, 2964, 1641, 1521, 1440 cm^{-1}; δ_H (400 MHz, $CDCl_3$): 7.13 (d, $J = 7$ Hz, 1H), 5.82–5.65 (m, 2H), 5.27–5.23 (m, 1H), 5.19–5.11 (m, 4H), 4.63–4.56 (m, 2H), 4.54–4.48 (m, 1H), 3.74 (s, 3H), 3.72–3.66 (m, 1H), 3.60–3.56 (m, 1H), 2.60–2.48 (m, 3H), 2.41–2.34 (m, 2H), 2.10–1.89 (m, 3H), 1.40 (s, 9H); δ_C (100 MHz, $CDCl_3$): 174.7, 171.8, 170.6, 150.3, 132.5, 132.2, 119.0, 118.9, 79.8, 59.8, 52.3, 52.0, 51.4, 47.4, 37.2, 36.2, 28.3, 27.2, 25.0; HRMS calcd. for $C_{21}H_{33}N_3O_6$ $[M - H]^-$ 422.2291, found 422.2299.

(3*S*,8*S*,13*aS*)-Methyl 8-(*tert*-butoxycarbonylamino)-1,9-dioxo-2,3,4,7,8,9,11,12,13,13*a*-decahydro-1*H*-pyrrolo[1,2-*a*][1,4]diazacycloundecine-3-carboxylate (9). Ring-closing metathesis of **8** (160 mg, 0.379 mmol) was carried out in a manner analogous to that used for the preparation of **4a** using Grubbs' ruthenium benzylidene catalyst (16 mg, 0.019 mmol) under a nitrogen atmosphere to afford **9** (145 mg, 97%) after flash column chromatography (EtOAc–petroleum spirit, 7 : 3). **9**: white solid; mp 134–137 °C; FT-IR (KBr) 3298, 2978, 1749, 1698, 1688, 1632 cm^{-1}; δ_H (400 MHz, $CDCl_3$): the spectrum was complex due to the presence of stereochemical and conformational isomers with up to four signals for each hydrogen. 7.43 (d, $J = 10.5$ Hz, *ca.* 0.4H), 7.00 (br, *ca.* 0.6H), 6.90–6.58 (m, *ca.* 1H), 5.64–5.53 (m, *ca.* 0.4H), 5.50–5.80 (m, *ca.* 1H), 5.13–5.03 (m, *ca.* 0.6H), 4.92–4.73 (m, *ca.* 1H), 4.68–4.40 (m, *ca.* 1.6H), 4.33–4.26 (m, *ca.* 0.4H), 3.80–3.38 (m, *ca.* 5H), 2.60–1.88 (m, *ca.* 7H), 1.82–1.70

(m, *ca.* 1H), 1.41 (s, 9H); δ_C (100 MHz, $CDCl_3$): 173.0, 172.4, 172.1, 171.8, 171.7, 171.0, 170.9, 170.8, 170.7, 170.6, 170.0, 169.2, 155.3, 155.2, 155.0, 154.9, 130.3, 129.5, 129.4, 128.6, 128.4, 128.2, 126.0, 125.1, 80.12, 80.0, 79.9, 58.4, 58.3, 58.1, 58.0, 53.2, 52.8, 52.7, 52.5, 52.4, 51.8, 51.7, 51.5, 51.1, 50.5, 47.0, 46.3, 45.6, 38.3, 36.2, 33.8, 33.4, 33.2, 31.0, 30.8, 29.3, 28.4, 25.2, 24.8, 24.7, 24.6, 24.3; HRMS calcd. for $C_{19}H_{29}N_3O_6$ $[M + H]^+$ 396.2134, found 396.2031.

(3*S*,8*S*,13*aS*)-Methyl 8-(*tert*-butoxycarbonylamino)-1,9-dioxo-dodecahydro-1*H*-pyrrolo[1,2-*a*][1,4]diazacycloundecine-3-carboxylate (10). The synthesis of **10** was carried out in a manner analogous to that used for the hydrogenation of **4a** (23.7 mg, 0.060 mmol) to obtain the desired compound (22.8 mg, 96%). **10**: colourless gum; FT-IR (film) 3442 (br), 2981, 1676, 1539, 1455 cm^{-1}; δ_H (400 MHz, $CDCl_3$): 7.30 (d, $J = 9$ Hz, 1H, NH2), 5.42 (d, $J = 7.5$ Hz, 1H, NH8), 5.01 (d, $J = 8$ Hz, 1H, H13a), 4.62–4.58 (m, 1H, H3), 4.48–4.44 (m, 1H, H8), 3.73 (s, 3H, OMe), 3.69–3.67 (m, 1H, H10), 3.51–3.46 (m, 1H, H10′), 2.50–2.44 (m, 1H, H12), 2.32–2.25 (m, 1H, H11), 2.08–1.93 (m, 2H, H7 and H11′), 1.88–1.77 (m, 2H, H4 and H12′), 1.66–1.56 (m, 2H, H4′ and H7′), 1.55–1.48 (m, 2H, H5 and H6), 1.43 (s, 9H, $C(CH_3)_3$), 1.38–1.36 (m, 1H, H6′), 1.27–1.20 (m, 1H, H5′); δ_C (100 MHz, $CDCl_3$): 173.4, 171.8, 170.2, 155.0, 79.7, 58.8, 52.6, 52.2, 51.9, 46.1, 29.7, 29.4, 28.3, 24.9, 23.8, 22.8, 21.6; HRMS calcd. for $C_{19}H_{31}N_3O_6$ $[M - H]^-$ 396.2135, found 396.2124.

Nuclear magnetic resonance spectroscopy

All NMR analyses of conformations were performed at 500 MHz on Bruker AMX500 or DRX500 spectrometers with sample temperatures regulated at either 298 K or 238 K. Proton resonance assignments were derived from the combined application of standard 2D NMR techniques[29] including g-COSY, TOCSY ($\tau_m =$ 80 ms) and multiplicity-edited HSQC. NOEs for peak assignments and for molecular modelling studies were obtained from Tr-ROESY experiments employing a phase alternating spin-lock to suppress TOCSY interference and with mixing times (τ_m) of 300–500 ms. NOE intensities were calibrated from volume integrals relative to that of a resolved geminal pair (distance 0.18 nm) and were classified as strong (<0.3 nm), medium (0.3–0.35 nm) and weak (>0.35 nm).[30] These distance ranges were employed when selecting energy minimised structures displaying inter-proton separations within these bounds.

Molecular modelling

Molecular modelling work was performed using the Sybyl suite of computer programs with the Tripos implementation of the MMFF94 force field used throughout.[31] Initially, a stochastic conformational search of each cyclic peptidomimetic was carried out to identify representative minimum energy conformers as follows. Initial molecular models were energy minimised (convergence criterion: RMS energy gradient < 0.001 kcal mol^{-1}/Å), and used as starting points for high temperature molecular dynamics simulations ($T = 2500$ K). In each case, a total of 500 samples were extracted from the dynamics trajectory at time intervals of 1 ps. These conformers were then energy minimised, and duplicate structures eliminated (match criterion: heavy atom RMSD < 0.2 Å). The final unique minimum-energy conformers were then sorted by energy. Conformer models satisfying experimental NOE intensities were identified by examining tables of proton–proton distances computed for the set of minimum energy structures derived from the search procedure. In a few cases, it was necessary to use an additional constrained minimisation followed by an unconstrained minimisation step to flip structures into minimum energy conformers that better satisfied the experimental data. This was because the initial conformational searches were not exhaustive.

Acknowledgements

We thank Dr M. A. McDonough for helpful discussions. This work was supported by the Biotechnology and Biological Sciences Research Council (BBSRC) and the Development and Promotion of Science and Technology Talents Project (DPST), Thailand (to M. K.).

Notes and references

1 S. Hanessian, G. McNaughton-Smith, H. G. Lombart and W. D. Lubell, *Tetrahedron*, 1997, **53**, 12789–12854.
2 L. Belvisi, L. Colombo, L. Manzoni, D. Potenza and C. Scolastico, *Synlett*, 2004, 1449–1471.
3 R. M. Freidinger, *J. Med. Chem.*, 2003, **46**, 5553–5566.
4 V. A. Kumar and K. N. Ganesh, *Acc. Chem. Res.*, 2005, **38**, 404–412.
5 L. Halab, F. Gosselin and W. D. Lubell, *Biopolymers*, 2000, **55**, 101–122.
6 G. Nemethy and M. P. Printz, *Macromolecules*, 1972, **5**, 755–758.
7 E. J. Milner-White, *J. Mol. Biol.*, 1990, **216**, 386–397.
8 J. M. Elkins, K. S. Hewitson, L. A. McNeill, J. F. Seibel, I. Schlemminger, C. W. Pugh, P. J. Ratcliffe and C. J. Schofield, *J. Mol. Biol.*, 2003, **278**, 1802–1806.
9 I. Alkorta and G. H. Loew, *Protein Eng.*, 1996, **9**, 573–583.
10 J. Yang and J. W. Quail, *Acta Crystallogr., Sect. D: Biol. Crystallogr.*, 1999, **55**, 625–630.
11 L. Kirnarsky, M. Nomoto, Y. Ikematsu, H. Hassan, E. P. Bennett, R. L. Cerny, H. Clausen, M. A. Hollingsworth and S. Sherman, *Biochemistry*, 1998, **37**, 12811–12817.
12 M. J. Yang, J. C. Culhane, L. M. Szewczuk, C. B. Gocke, C. A. Brautigam, D. R. Tomchick, M. Machius, P. A. Cole and H. T. Yu, *Nat. Struct. Mol. Biol.*, 2007, **14**, 535–539.
13 M. E. Cockman, D. E. Lancaster, I. P. Stolze, K. S. Hewitson, M. A. McDonough, M. L. Coleman, C. H. Coles, X. H. Yu, R. T. Hay, S. C. Ley, C. W. Pugh, N. J. Oldham, N. Masson, C. J. Schofield and P. J. Ratcliffe, *Proc. Natl. Acad. Sci. U. S. A.*, 2006, **103**, 14767–14772.
14 M. L. Coleman, M. A. McDonough, K. S. Hewitson, C. Coles, J. Mecinovic, M. Edelmann, K. M. Cook, M. E. Cockman, D. E. Lancaster, B. M. Kessler, N. J. Oldham, P. J. Ratcliffe and C. J. Schofield, *J. Biol. Chem.*, 2007, **282**, 24027–24038.
15 D. Lando, D. J. Peet, J. J. Gorman, D. A. Whelan, M. L. Whitelaw and R. K. Bruick, *Gene Dev.*, 2002, **16**, 1466–1471.
16 K. S. Hewitson, L. A. McNeill, M. V. Riordan, Y. M. Tian, A. N. Bullock, R. W. Welford, J. M. Elkins, N. J. Oldham, S. Bhattacharya, J. M. Gleadle, P. J. Ratcliffe, C. W. Pugh and C. J. Schofield, *J. Biol. Chem.*, 2002, **277**, 26351–26355.
17 P. C. Mahon, K. Hirota and G. L. Semenza, *Gene Dev.*, 2001, **15**, 2675–2686.
18 C. J. Schofield and P. J. Ratcliffe, *Nat. Rev. Mol. Cell Biol.*, 2004, **5**, 343–354.
19 S. Hanessian and M. Angiolini, *Chemistry*, 2002, **8**, 111–117.
20 T. M. Trnka and R. H. Grubbs, *Acc. Chem. Res.*, 2001, **34**, 18–29.
21 S. H. Gellman, G. P. Dado, G. B. Liang and B. R. Adams, *J. Am. Chem. Soc.*, 1991, **113**, 1164–1173.
22 A. Pardi, M. Billeter and K. Wuthrich, *J. Mol. Biol.*, 1984, **180**, 741–751.

23 B. E. Fink, P. R. Kym and J. A. Katzenellenbogen, *J. Am. Chem. Soc.*, 1998, **120**, 4334–4344.
24 W. Kabsch and C. Sander, *Biopolymers*, 1983, **22**, 2577–2637.
25 A. Lindemann, V. Kinzel, P. Rosch and J. Reed, *Proteins*, 1997, **29**, 203–211.
26 L. Belvisi, A. Bernardi, L. Manzoni, D. Potenza and C. Scolastico, *Eur. J. Org. Chem.*, 2000, 2563–2569.
27 S. Isokawa, M. Narita and K. Umemoto, *Makromol. Chem.*, 1993, **194**, 3247–3259.
28 B. Odell, S. J. Hammond, R. Osborne and M. W. Goosey, *J. Comput. Aided Mol. Des.*, 1996, **10**, 89–99.
29 T. D. W. Claridge, *High-Resolution NMR Techniques in Organic Chemistry*, Pergamon, Oxford, 1999.
30 D. Neuhaus and M. P. Williamson, *The Nuclear Overhauser Effect in Structural and Conformational Analysis*, Wiley-VCH, New York, 2nd edn, 2000.
31 *SYBYL 7.2*, Tripos International, 1699 South Hanley Rd, St. Louis, Missouri, 63144, USA.